# Aperture Synthesis Observations of Orion-KL in CS lines and 3mm Continuum.

Y. MURATA[1], R. KAWABE[2], M. ISHIGURO[2], T. HASEGAWA[3], AND M. HAYASHI[1]

[1] Department of Astronomy, University of Tokyo
[2] Nobeyama Radio Observatory, National Astronomical Observatory
[3] Institute of Astronomy, University of Tokyo

**Summary:** We have made aperture synthesis maps toward the Orion-KL nebula in CS(1-0), CS(2-1) and 3mm continuum with the Nobeyama Millimeter Array (NMA). The CS(1-0) maps were obtained across the central 2′ region of the Orion-KL nebula. Our maps show the rotating disk around the KL nebula with the diameter of 0.3 pc and the mass of 25 $M_\odot$. The disk clearly shows the Keplerian rotation, which indicates that the mass of the KL nebula is 100 – 150 $M_\odot$. The shell structure around the molecular outflow is also found in CS(1-0) map. This structure also appears in CS(2-1) map.

From 3mm continuum map, we have found at least six continuum sources. One of them is f-f emission from the ultra-compact HII region around BN. Other sources are the dust clumps whose masses are estimated to be 1 – 4 $M_\odot$. The distribution of the dust clumps shows clear anti-correlation with the 20 $\mu$m emissions. This indicates that the 20 $\mu$m emissions are obscured by these dust clumps.

## 1. Introduction

The Orion-KL nebula is a massive star forming region which has been studied extensively (Genzel and Stutzki 1989). It is certain that IRc2 is the central star of this region from observations concerning the outflow (Genzel *et al.* 1981; Wright *et al.* 1983). Around the Orion-KL nebula, we can see the typical structures of young stellar objects. These are the bipolar molecular outflow (Erickson *et al.* 1981) and the rotating disk perpendicular to the axis of the outflow (Plambeck *et al.* 1982; Hasegawa *et al.* 1984; Vogel *et al.* 1985). We have made CS observations for the Orion-KL nebula with NMA, to understand the detailed structure and dynamics of this region. A 3 mm continuum map have been also obtained at the same time.

## 2. Observations

The CS(J=1-0),(2-1) lines and 3mm continuum were observed with the Nobeyama Millimeter Array (NMA; Ishiguro *et al.* 1984). We used IRc2 as the phase center for the observation. The front-end receivers were the dual-channel SIS receivers, whose typical system noise temperature are 300 K at 49 GHz and 400 K at 98 GHz. The back-end was a digital FFT spectro-correlator (FX), which has 1024 frequency channels. The CS(1-0) observations were carried out from 1988 March to 1989 April with 7 array configurations. The synthesized beam had an angular size of 6″ × 8″ (FWHM), and the primary beam size was 140″. The bandwidth of FX was 80 MHz, giving a velocity resolution of 0.48 km $s^{-1}$. The CS(2-1) and 3mm continuum observations were carried out from 1989 December to 1990 March with 4 configurations. The synthesized and primary beam size were 2″ × 3″ and 70″, respectively. The bandwidth of FX was 320 MHz, giving a velocity resolution of 0.96 km $s^{-1}$. The total bandwidth for the continuum observation was 250 MHz.



*E. Falgarone et al. (eds.), Fragmentation of Molecular Clouds and Star Formation,* 357–360.

The bandpass calibration was made from the observation of 3C84 or 3C273. The visibility gain calibration was made with 0605-085, assuming its flux density of 3.2 Jy at 48 GHz, and 1.8 Jy at 98 GHz.

## 3. Disk with Keplerian rotation

Figure 1 shows the spatial distributions of the CS(1-0) emission in the LSR velocity ranges of 5.5 – 12.2 km $s^{-1}$. Three features are prominent in Fig. 1: (*1*) a strong compact source at the center, corresponding to the hot core, (*2*) the large rotating disk around Orion-KL, which is seen as the elongated structure from northeast to the southwest, and (*3*) two ridges extending toward the northwest and perpendicular to the disk.

The disk has the diameter of 0.3 pc and the thickness of 0.03 pc. The density of this disk is $\sim 10^5$ $cm^{-3}$ derived by LVG model (Linke and Goldsmith 1980) using the CS(2-1) data (Mundy *et al.* 1988). The gas kinetic temperature was assumed to be $\sim$ 40 K derived from the $CH_3CN$ results (Andersson 1985). The total mass of the disk component is $\sim$ 25 $M_\odot$ assuming the disk structure. The disk is seen as the elongated structure with the position angle of 30°. There is a weaker CS emitting region in a few arcsecond northeast of IRc2, which divide the disk to NE and SW parts. The center line of the disk are shown in Fig. 1.

We made a position-velocity map along the center line of the disk (Figure 2). The center position is the nearest point to IRc2. The hot core shows the broad line emission ($\gtrsim$ 20 km $s^{-1}$) in $0'' - -20''$ from the center. The other part in this map corresponds to the disk component. The Keplerian rotation curves with the central mass of 50, 100, 150, and 200 $M_\odot$ are shown in Fig. 2, for the systemic velocity of $V_{LSR}$ = 8.5 km $s^{-1}$. When considering about the effects of the random gas motion ($\sim$ 0.5 – 1.0 km $s^{-1}$), the rotation of the outer disk is well fitted by the Keplerian motion with the central mass of between 100 – 150 $M_\odot$.

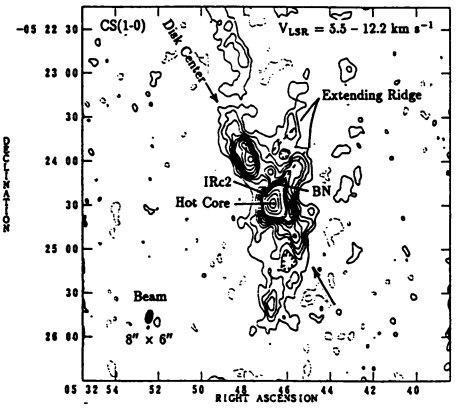


**Figure 1** Map of the average emission in the CS (1-0) line in the velocity interval 5.5 < $V_{LSR}$ < 12.2 km $s^{-1}$. Thick lines indicate the center of the disk.

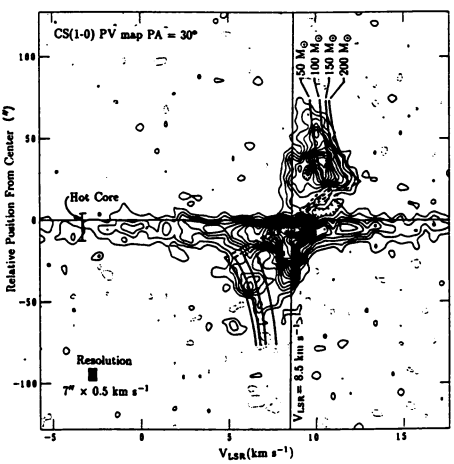


**Figure 2** Position Velocity map of the CS disk. Thick lines show the Keplerian rotation curve for each central masses.

https://doi.org/10.1017/S0074180900199061 Published online by Cambridge University Press

The motion in the inner part of the disk ($r < 25''$) departs from the Keplerian rotation, and has no high velocity gas motion except for the hot core. This indicate that there is no CS emission in the center of the disk. The SO expanding ring (Plambeck *et al.* 1982) and the proper motion of $H_2O$ masers correspond to inner edge of the disk. These observational results indicates that the dynamics of the molecular gas change dramatically at the inner edge of the disk. Therefore, the shock surface is expected to exist between rotating disk and expanding ring.

## 4. Shell structures around the molecular outflow

Two ridges in Fig. 1 correspond to the CS shell in previous result (Murata *et al.* 1989). The extension is about $30'' - 40''$ and the southern ridge (extending from the hot core emission) is stronger than the northern one. The molecular outflow is confined between these two ridges.

We can also see these structures in CS(2-1) map in $V_{LSR} = 9.5 - 11.4$ km s$^{-1}$ (Figure 3) with the resolution of $2'' \times 3''$. Because the resolution is twice as high as that of CS(1-0) map, we can resolve some clumps on the shell. The shell is surrounding the molecular outflow like as CS(1-0). The $H_2$ emissions in this region is the evidence of the shock between the outflow and the ambient gas (Beckwith *et al.* 1978). These results support the hydrodynamical models of molecular outflows that high velocity winds accelerate neutral gas which in turn sweeps up the ambient material to form a shock-compressed shell (Königl 1982).

Two $NH_3$ filaments are located on the extension of the ridges in Figure 1. This means that the high velocity winds expand out through the CS shell (or extending ridge) toward the directions along which the $NH_3$ filaments and the HH objects are formed (Murata *et al.* 1990).

## 5. Continuum sources at $\lambda$ 3mm

Figure 4 shows the map of the $\lambda$3mm continuum with $2'' \times 3''$ resolution. Six clumps (A–F) are identified. The clump A corresponds to BN object. The flux density of the clump A is consistent with that of f-f emission from the ultra compact HII region around BN, whose spectrum was proposed from the lower frequency observations by Moran *et al.* (1983).

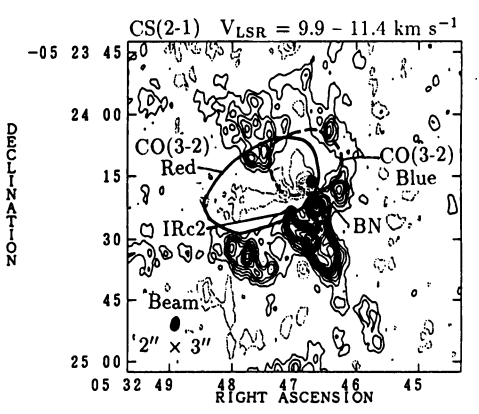


**Figure 3** Map of the average emission in the CS (2-1) line in the velocity interval $9.5 < V_{LSR} < 11.4$ km s$^{-1}$. Thick solid and broken lines show the molecular outflow observed in CO (3-2) (Erickson *et al.* 1982)

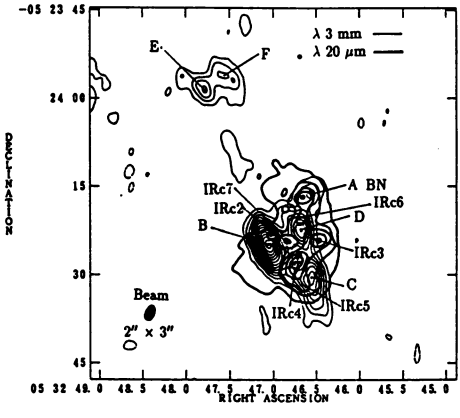


**Figure 4** Map of the 3 mm and 20 $\mu$m (Dowens *et al.* 1981). A–F are the identified 6 clumps.

https://doi.org/10.1017/S0074180900199061 Published online by Cambridge University Press

Though the other clumps are more intense than the clump A, they have not detected at lower frequency (Garay, Moran and Reid 1987). Therefore, the emissions of these five clumps come from the dust. The parameters of the clumps are in table 1. The mass and the optical depth is derived following the appendix in Mezger *et al.* (1990). Typical mass and size of the clumps are 1–3 $M_\odot$ and $4'' - 7''$, respectively.

We compared the distribution of these dust clumps with the 20 $\mu$m continuum map (Downes *et al.* 1981; Fig. 4). The maps show clear anti-correlation between 20 $\mu$m and 3 mm continuum emissions. Though the optical depth of the dust is small ($\sim 10^{-2}$) at $\lambda$ 3 mm, these clumps will become optically thick at 20 $\mu$m. This anti-correlation indicates that the dust clumps obscure the 20 $\mu$m emission reflecting the radiation from IRc2 and BN.

**Table 1:** Parameters of clumps.

| Clumps | Size ($''$) | Flux (mJy) | Mass* ($M_\odot$) | $\tau_{3mm}$* ($\times 10^{-3}$) |
|---|---|---|---|---|
| A(BN) | 4.2 × 4.0 | 52 | — | — |
| B | 7.6 × 4.0 | 370 | 3.7 | 7.4 |
| C | 7.8 × 4.7 | 260 | 2.6 | 4.3 |
| D | 6.3 × 4.5 | 207 | 2.1 | 7.3 |
| E | 4.0 × 3.0 | 70 | 0.7 | 3.5 |
| F | 5.2 × 5.5 | 124 | 1.2 | 2.7 |
| B+C+D | ——— | 836 | 8.4 | 6.2 |

* Assuming $T_d = 200$ K, $\tau \propto \lambda^{-2}$.

## References


Andersson,M. 1985, Proc. on "(Sub)Millimeter Astronomy", pp353.

Beckwith,S., Persson,S.E., Neugebauer,G.,and Becklin,E.E. 1978, *Ap. J.*, **223**, 464.

Downes,D., Genzel,R., Becklin,E.E., and Wynn-Williams,C.G. 1981, *Ap. J.*, **244**, 869.

Erickson,N.R. *et al.* 1982, *Ap. J.(Letters)*, **261**, L103.

Garay,G., Moran,J.M., and Reid,M.J., 1987, *Ap. J.*, **314**, 535.

Genzel,R., Reid,M.J., Moran,J.M., and Dowens,D. 1981, *Ap. J.*, **244**, 884.

Genzel,R., and Stutzki,J., 1989, *Ann. Rev. Astr. Ap.*, **27**, 41.

Hasegawa,T. *et al.* 1984, *Ap. J.*, **283**, 117.

Ishiguro,M. *et al.* 1984, in *Proc. Int. Symp. of Milli-meter and Submillimeter Wave Radio Astronomy*, ed. J.Gomez-Gonzales (Granada:URSI), p.75

Königl,A. 1982, *Ap. J.*, **261**, 155.

Linke,R.A., and Goldsmith,P.F., 1980, *Ap. J.*, **235**, 437.

Mezger,P.G., Wink,J.E., and Zylka,R. 1990, *Astr. Ap.*, **228**, 95.

Moran,J.M.*et al.* 1983, *Ap. J.(Letters)*, **271**, L31.

Mundy,L.G. *et al.* 1988, *Ap. J.*, **325**, 382.

Murata,Y., *et al.* 1989, in *Structure and Dynamics of the Interstellar Medium, IAU Coll. No 120*, ed. G.Tenorio-Tagle, M.Moles, and J.Melnick, (Berlin:Springer), pp.327

Murata,Y. *et al.* 1990, *Ap. J.*, in press.

Plambeck,R.L. *et al.* 1982, *Ap. J.(Letters)*, **259**, 617.

Vogel,S.N., Bieging,J.H., Plambeck,R.L., Welch,W.J., Wright,M.C.H. 1985, *Ap. J.*, **296**, 600.

Wright,M.C.H. *et al.* 1983, *Ap. J.(Letters)*, **267**, L41.

Wynn-Williams,C.G., Genzel,R., Becklin, E.E., and Downes,D. 1984, *Ap. J.*, **281**, 172.